CI&CEQ
Chemical Industry & Chemical Engineering Quarterly

Available online at
Association of the Chemical Engineers of Serbia AChE
www.ache.org.rs/CICEQ

Chem. Ind. Chem. Eng. Q. 30 (2) 123–133 (2024) CI&CEQ

KADHUM AUDAA JEHHEF[1]
MUSAAB KADEM RASHEED[2]
MOHAMED ABED AL ABAS SIBA[2]

[1]Technical Engineering College, Baghdad, Middle Technical University, Baghdad, Iraq

[2]Institute of Technology, Middle Technical University, Baghdad, Iraq

NUMERICAL SIMULATION OF THE OSCILLATING THIN PLATE IMPACT ON NANOFLUIDS FLOW IN CHANNEL

Article Highlights

- The titled oscillating thin plate inside the flow direction increases pressure drop
- The pressure increased from 2.61 to $6.21 \cdot 10^3$ Pa when increasing the plate angle from 30 to 90°
- The Nusslet number increases by 8% when decreasing the angle from 90° to 60° near the thin plate
- Increasing the inclined angle from 30° to 90°, the maximum drag force increased from 220 to 850 N/m

Abstract

The present numerical study aims to present the effect of a titled oscillating thin plate with different inclination angles on the Al_2O_3-water nanofluid flow and heat transfer performance. The subsequent work establishes methods for forming fluid-structure interactions by the impact of Al_2O_3-water nanofluid at 0.1-1.0 vol. % volume fraction upon the thin plate using COMSOL Multiphysics 5.4. The turbulent model is solved using the (k-ε) model, and the flow assembly around the thin plate obstacle has been confirmed at the Reynolds number of $Re=4\times10^4$. It exemplifies how Nanofluid flow interaction can distort structures. The turbulent, two-dimensional, stationary, and incompressible flow around an oscillating thin plate with inclined angles with upstream and downstream mounted inside a horizontal channel was studied. The numerical study includes an investigation of the effect of five inclination angles of the thin plate (30, 60, 90, 120, and 150°) on the pressure, velocity, and temperature contours of the Al_2O_3-water nanofluid. Also, the study presented the drag profile and left a force on the thin plate caused by the fluid flow. The results showed that a titled oscillating thin plate inside the flow direction increases pressure drop, von Mises deformation stress, x-displacement and drag force fields, and the Nusselt number. Where the pressure increased from 2.61×10^3 to 6.21×10^3 pa, the von Mises stress increased from 4.43×10^6 to 1.78×10^7 N/m, and the X-displacement increased from 1.6 to 5.5 mm when increasing the plate angle from 30 to 90°.

Keywords: fluid-structure interactions, Lagrangian-Eulerian (ALE) technique, Multiphysics, nanofluid.

SCIENTIFIC PAPER

UDC 51:53:66

The study of the hydrodynamic forces behavior on thin plates can oscillate in relation to the regimes of observable flow. Many quantitative and qualitative researches on the flow arrangements were used to classify the corresponding performance of the hydrodynamic forces. Investigate the flow rate patterns in the variety enclosed performance of zones of diverse flowrate and study the influence of these flow rates on the fluid pressure of thin plate upstream flow. Among much experimental research alarmed with solid structures with sharp edges, the effect of solid flat plates on the aerodynamic characteristics at various attack inclinations in an oscillatory movement was

Correspondence: M.K. Rasheed, Institute of Technology, Middle Technical University, Baghdad, Iraq.
E-mail: musaabk.rasheed@mtu.edu.iq
Paper received: 1 April, 2023
Paper revised: 12 June, 2023
Paper accepted: 23 June, 2023

https://doi.org/10.2298/CICEQ230401017J

considered by Okajima *et al.* [1].

Carberry *et al.* [2] studied a circular cylinder at $Re < 10^4$ to measure the effect of the circular cylinder's presence on the sinusoidal oscillations transverse to a uniform stream. Outcomes showed several performances of fluid action and transitions passed through the Strouhal frequency would change only slightly during the transition. Sarpkaya [3] examined the simple examination to achieve the limitations of monitoring the crosswise vibration by vortex-induced of the rigid cylinder. The limitations as the density of the fluid, flow speed, cylinder length, cylinder diameter, spring constant, and structural damping factor were studied. Mao *et al.* [4] explored the flow oscillating near the parallel plates placed in a vertical wave resonator. As a result, the Reynolds number vagaries, a range of distinct flow patterns is reported for the fluid being expelled from the stack.

Dahl [5] specified the flow of natural instability that happens at the frequency of Strouhal. The vortex frequency detaching will be associated with the frequency of structural oscillation when the structure (body) moves. The results showed that the frequency band grows, accumulated in the amplitude of fluid motion. Lee and Allen [6] detected that softer structures take a wider “lock-in” band than harder solid constructions. Therefore, the parameters of mass, stiffness, and damping of interest control the response amplitude.

Amandolèse and Hémon [7] used a square tube in the flow of the storm channel. The free vibrations indicated the self-excited vibration. Numerous donations have been made to increase the kinematics of vibrations of self-excited solid cylinders. Yang [8] examined a bluff structure placed in a fluid flow by subjecting it to VIV. The VIV is a flat plate oscillation with a lone rotating notch of freedom. The result specified that reverberation seems a huge rejoinder bounty happens in the “lock-in” region. Lam *et al.* [9] used FSI (Fluid Structure Interaction) of cylindrical structures to examine the meaningful advance in understanding unsteady phenomena. The occurrence of structures with sharp edges can meaningfully change the behavior of fluid flow problems by viscous layer departure. Shrestha *et al.* [10] accessible a trial investigation on plate oscillations flooded in a Newtonian fluid. The FSI tricky is examined by particle image velocimetry (PIV). The results showed the association between vortex shedding and flow physics.

Zhang and Ishihara [11] calculated the coefficients of the hydrodynamic of multiple plates in fluctuating streams. LES (Large eddy simulations) of fluid with the finite volume method is used to calculate the fluid forces on oscillated plates. Sun *et al.* [12] investigated the effect of flow-induced vibration (FIV) caused by a deformable fin on the convective heat exchange mechanism. Also, the properties of heat transmission for various fin rigidity combinations were studied. The results showed that forced convection heat transfer can significantly increase when the fin exhibits large-amplitude oscillation. Yaseen and Ismael [13] focus on how a baffle designed to improve heat transmission in an open trapezium filled with non-Newtonian fluid deflects. A parallel plate channel and a trapezoidal cavity make up the computational domain. A flexible baffle is hung on the channel's top wall, with its free end pointing toward the cavity's center. The flow in the channel and the convective currents are affected by the baffle's interactions.

Ram *et al.* [14] offered a mathematical model to examine non-Newtonian Casson fluid flow in the presence of radiation, thermo-diffusion, and Ohmic dissipation over an infinite vertical plate domain. The results showed that magnetic and radiation fields increased heat distribution and improved yield stress through an enhancement in the Casson term decreased the flow speed. Usman *et al.* [15] discussed the heat transfer in the Williamson fluid flow, in a ciliated channel with a magnetic field and porous medium. The intended problem mathematical model complicates the PDE system in different dissipation. The conduction process escalated the heat transfer through the liquid molecules.

Shamshuddin *et al.* [16] studied the influence of Hall current, heat source, and Soret number in a rotating channel by describing three-dimensional mixed convection flow with convective mass and heat transfer on a squeezing nanofluid. Material properties were studied by deploying a nanoscale formulation with the Tiwari-Das model. The findings show that the squeezing term enhances the flow rate motion but decreases species diffusion and nanoparticle conductivity. Salawu *et al.* [17] investigated theoretically the thermal ignition and double exothermic combustible reaction for a viscous liquid in a channel. The flow is propelled by the upper wall motion, reaction activation energy, and pre-exponential chemical kinetics that activate the inner temperature. The dimensionless viscoelastic exothermic reaction model solutions are obtained by integrating collocation-weighted residual techniques. Shamshuddin *et al.* [18] presented a theoretical study on a micropolar fluid medium channel in mixed and nonlinear convection with the assumptions of reactive agent species and thermal radiation. It was found that the concentration, dimensionless velocity, and temperature of the micropolar fluid have a maximum value at the center of the channel.

A few works studied the interaction between the nanofluid flow and the titled movable thin plate. This work is dedicated to the problem of harmonic oscillations of titled thin plates with numerous inclination angles using a viscous incompressible nanofluid. Also, the two-dimensional flows caused by the plate oscillations and their hydrodynamic effect on the plates were investigated. The fluid motion is described by the non-stationary Navier-Stokes equations, which are solved numerically based on the finite volume method. The simulation is carried out for plates with different angles of control parameters of the oscillatory process. The analysis of the flow hydrodynamic effects on the plates allows the establishment of new effects associated with the influence of the shape on the drag and inertia forces. The present numerical simulation focused on the effect of oscillating thin plate inclination angles on the hydrodynamic forces and heat transfer of Al_2O_3-water nanofluid at 0.2-1.0 vol.% volume fraction flow upon the thin plate using COMSOL Multiphysics 5.4.

METHODOLOGY AND ANALYSIS

Model geometry

The present model includes a thin plate as an obstacle and a narrow vertical structure that achieved in the middle of a horizontal flow channel as a model geometry as presented in Fig.1. Al_2O_3-water nanofluid flow inlets to the horizontal flow channel as a fully developed flow from the left of the channel and exit from the right and the Al_2O_3-water nanofluid flow will strike the obstacle flat plate powers the fluid flow paths toward the upper part of the duct. The thin plate structure was made from a deformable material that will bend under the applied force of the moving fluid. The dimension of the flow channel chosen as the channel length is 100 cm and the channel height is 10 cm and the plate length is 5 cm, and the thin plate thickness is 1 cm.

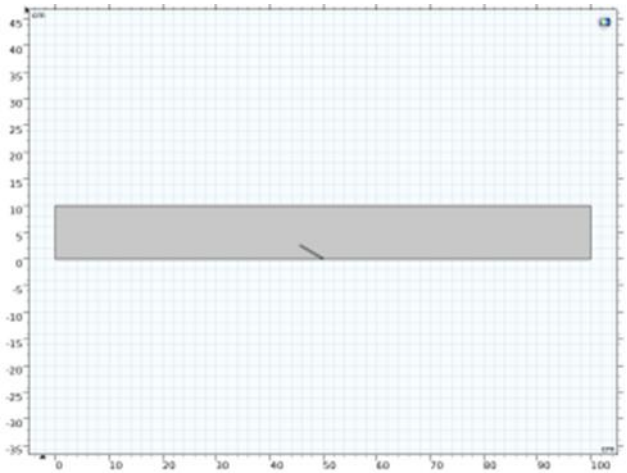

Figure 1. Model geometry of flow domain of present problem (all dimensions in cm).

Governing Equations

Fluid deformed mechanics

The Al_2O_3-water nanofluid current in the duct flow is defined using the equations of Navier-Stokes of pressure (p) and velocity u = (u, v) in the coordinate of deformed moving as follows:

Mass conservation equation:

$$\nabla u = 0 \tag{1}$$

Momentum conservation equation:

$$\rho\frac{\partial u}{\partial t} - \nabla\cdot\left[-pI + \eta\left(\nabla U + (\nabla U)^T\right)\right] + \rho\left((u-u_m)\cdot\nabla\right)u = F \tag{2}$$

Energy equation:

$$\frac{\partial}{\partial t}(\rho E) + \nabla\left(\vec{v}(\rho E + p)\right) = \nabla\left[k_{eff}\nabla T - \sum_j h_j J_j + \left(\overline{\overline{\tau}}\vec{v}\right)\right] + S_h \tag{3}$$

Assume that no gravitation that affects the Al_2O_3-water nanofluid F = 0.

Turbulent kinetic energy

$$\frac{\partial uk}{\partial x} + \frac{\partial vk}{\partial y} = \frac{1}{\rho}\frac{\partial}{\partial x}\left[\left(\mu + \frac{\mu_t}{\sigma_k}\right)\frac{\partial k}{\partial x}\right] + \frac{1}{\rho}\frac{\partial}{\partial y}\left[\left(\mu + \frac{\mu_t}{\sigma_k}\right)\frac{\partial k}{\partial y}\right] + \frac{1}{\rho}(G_k - G_b) - \varepsilon \tag{4}$$

Dissipation rate (Ɛ)

$$\frac{\partial u\varepsilon}{\partial x} + \frac{\partial v\varepsilon}{\partial y} = \frac{1}{\rho}\frac{\partial}{\partial x}\left[\left(\mu + \frac{\mu_t}{\sigma_\varepsilon}\right)\frac{\partial \varepsilon}{\partial x}\right] + \frac{1}{\rho}\frac{\partial}{\partial y}\left[\left(\mu + \frac{\mu_t}{\sigma_\varepsilon}\right)\frac{\partial \varepsilon}{\partial y}\right] + C_1\frac{\varepsilon}{\rho k}(G_k + C_3G_b) - C_2\frac{\varepsilon^2}{k} \tag{5}$$

Where μ_{eff} is effective viscosity coefficient

$$\mu_{eff} = \mu + \mu_t \tag{6}$$

Γ_{eff} is effective diffusion coefficient

$$\Gamma_{eff} = \frac{\mu}{p_r} + \frac{\mu_t}{\sigma_t} \tag{7}$$

μ_t is turbulent viscosity

$$\mu_t = \rho C_\mu\frac{k^2}{\varepsilon} \tag{8}$$

$$S_u = -\frac{2}{3}\frac{\partial k}{\partial x} \tag{9}$$

$$S_v = g\beta(T_f - T_{in}) \tag{10}$$

G_k is kinetic energy generation by shear

$$G_k = \mu_t \left(2\left[\left(\frac{\partial u}{\partial x}\right)^2 + \left(\frac{\partial v}{\partial y}\right)^2 \right] + \left(\frac{\partial u}{\partial y} + \frac{\partial v}{\partial x}\right)^2 \right) \quad (11)$$

G_b is kinetic energy generation by buoyancy

$$G_b = \frac{\mu_t}{\sigma_t} \frac{\partial T}{\partial y} g\beta \quad (12)$$

where "Cμ " is the value of an empirical constant for a flow with a high Reynolds number. The working fluid is air, which has a Prandtl number of (0.7) and produces a uniform heat flux on the absorber wall. The values of constants in the (K–Ɛ) models are presented in Table.1.

Table 1. Values of constants in the (K–Ɛ) models [15].

C μ	C_1	C_2	C_3	σ_ε	σ_k
0.09	1.44	192	1.0	1.3	1.0

Local heat transfer coefficient (h_x)

$$h_x = \frac{k_f \left(\partial T / \partial y \right)_{y=0}}{(T_s - T_b)} \quad (13)$$

Local Nusselt number can be calculated from:

$$\overline{Nu}_x = \frac{h_c D_h}{K_f} = -\frac{1}{\theta_w} \frac{\partial \theta}{\partial \overline{n}} \quad (14)$$

The mean Nusselt number can be calculated from:

$$\overline{Nu}_m = \frac{1}{A} \int_A Nu_x dx \quad (15)$$

To demonstrate the desired techniques, the following assumption will be illustrated:

1. Turbulent fluid flow.
2. Two-dimensional.
3. Stationary and incompressible flow around an oscillating thin plate.
4. Assume that the structure is long in the direction perpendicular to the image.
5. Assume the structure consists of a flexible material with a density ρ = 7850 kg/m^3 and Young's modulus E = 200 kPa.

Assume that no gravitation or other volume forces affect the fluid so that F = 0.

Solid structural mechanics

Deformations of the solid structure are resolved through nonlinear geometry formulation and an elastic preparation to agree with the deformations of the solid. The thin plate hitch is attached at the bottom side of the bottom wall of the fluid flow duct. All other object borders involved a weight of the Al_2O_3-water nanofluid flow is given by:

$$F_T = -n\left(-pI + \eta\left(\nabla u + (\nabla u)^T\right)\right) \quad (16)$$

where n is the normal vector on a flat plate. This force denotes the sum of the viscous and pressure forces in the nanofluid flow.

Boundary conditions

At the left-hand of the inflow of the inlet of the duct boundary, the flow is considered laminar flow and fully developed at the inlet of the duct with a parabolic profile velocity. The velocity grows and gets its peak value at 0.215 and then falls to 5 cm/s, representing a steady-state value. The velocity at the centerline in the x-axis (u_{in}) comes from:

$$u_{in} = \frac{Ut^2}{\sqrt{\left(0.04 - t^2\right)^2 + (0.1t)^2}} \quad (17)$$

At the right-hand of the outflow of the channel, the boundary condition is p = 0. At the channel's top and bottom solid walls (non-deforming boundary condition), the no-slip boundary conditions are imposed: u = 0, v = 0.

At the top and sides of the thin plate's solid (deforming) walls and on the deforming, the deformation velocities boundary conditions are $u_0 = u_t$ and $v_0 = v_t$.

The fixed boundary was chosen at the thin plate's bottom solid (deforming) wall. The working fluid (Al_2O_3-water nanofluid) flows through it with various flow rates (1, 3, 5, and 7 LPM). Fig. 2 demonstrates the nanofluid channel's physical model and boundary state with an oscillating thin plate. More information for the BC (Boundary condition) was implemented in statistical models and inclined thin plates to analyze the energy balance of the main components.

Thermophysical properties of nanofluids

Introducing the volume fraction of Nanofluid, the thermophysical properties of the Nanofluid (density and heat capacity) have been estimated from the pure fluid and Nanoparticle properties at the ambient temperature. The thermophysical properties of nanofluids used in the present study are for a mixture of the water and Al_2O_3, CuO, and TiO_2 nanoparticles with a diameter of 20 nm. The values of density, specific heat, dynamic viscosity, and thermal conductivity for the base fluid and considered nanoparticles were reported in table.2. Also, the solid properties of the steel

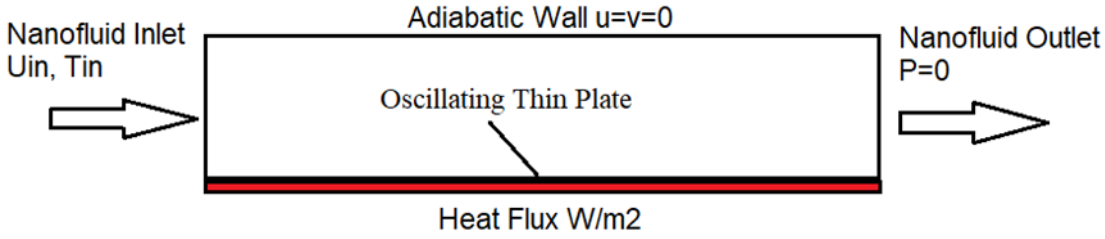

Figure 2. Geometry distribution and boundary conditions.

used in pore-level simulations were listed in Table 3. In the present study, a single-phase model is adopted, and the following equations are used to compute the thermal-physical properties of considered nanofluids.

Table 2. Water and Nanofluid properties used in present simulations [19].

Fluid properties	Water	Al_2O_3-nanofluids
ρ [Kg/m^3]	997.0	1057.17
μ [Kg/m. s]	8.899E-4	0.00169
Cp [J/Kg. k]	4181.7	3526.68
k [W/m. k]	0.6069	0.441

Table 3. Solid properties of the steel used in pore-level simulations [19].

Properties	Steel
Density [Kg/m^3]	7850
Young's modulus E [Pa]	2×10^5
Poisons ratio $^{\nu}$ [-]	0.33

Density

Equation of general relationships used to compute the effective density for a classical two-phase mixture given by Pak and Cho [19]:

$$\rho_{nf} = \varnothing\rho_p + (1-\varnothing)\rho_f \tag{18}$$

Specific heat

Calculation of the effective specific heat of nanofluid is straightforward. It can be based on the physical principle of the mixture. The specific heat is calculated from general relationships used to compute the effective specific heat at the reference temperature (T_{in}) for a classical two-phase mixture [20]:

$$Cp_{nf} = \frac{\varnothing\rho_p Cp_p + (1-\varnothing)\rho_f Cp_f}{\rho_{nf}} \tag{19}$$

Thermal expansion

Equation of general relationships used to compute the effective thermal expansion at the reference temperature (T_{in}) for a classical two-phase mixture given by Maiga *et al.* [21]:

$$B_{nf} = \frac{\varnothing\rho_p B_p + (1-\varnothing)\rho_f B_f}{\rho_{nf}} \tag{20}$$

Dynamic viscosity

The effective viscosity is calculated with the Einstein equation, which applies to spherical particles in volume fractions of less than 5.0 vol.% and is defined as follows [22]:

$$\mu_{nf} = \frac{\mu_f}{(1-\varnothing)^{2.5}} \tag{21}$$

Thermal conductivity

For particle-fluid mixtures, numerous theoretical studies have been conducted dating back to the classical work of Maxwell [23]. The effective thermal conductivity of the fluid can be determined by Maxwell-Garnett's (MG) model). For the two-component entity of spherical-particle suspension, the MG model gives:

$$k_{nf} = \left[\frac{k_p + 2k_f - 2\varnothing(k_f - k_p)}{k_p + 2k_f + \varnothing(k_f - k_p)}\right]k_f \tag{22}$$

Maxwell's formula shows that nanofluids' effective thermal conductivity relies on the spherical particle's thermal conductivity, the base fluid, and the volume fraction of the solid particles.

Solution method

The governing equations of Navier-Stokes are analyzed and explained on the mesh of a movable deformed flat plate of the commotional field, which establishes the Al_2O_3-water nanofluid flow. The mesh deformation is compared to the field's initial solid flat plate shape, calculated using the Hyperelastic smoothing method. The nearby and insider mesh of the moving plate will track the plate deformations. However, the flat plate deformation is fixed at zero in all instructions at the exterior boundaries of the nanofluid flow field. The method of Lagrangian- Eulerian adjustments the dynamic forces of the flat plate's deforming structure and the moving grid's

moving boundaries. COMSOL Multiphysics was used to investigate the systematization of the new mesh based on the solid flat plate structure's movement with mesh smoothing, as shown in Fig. 3.

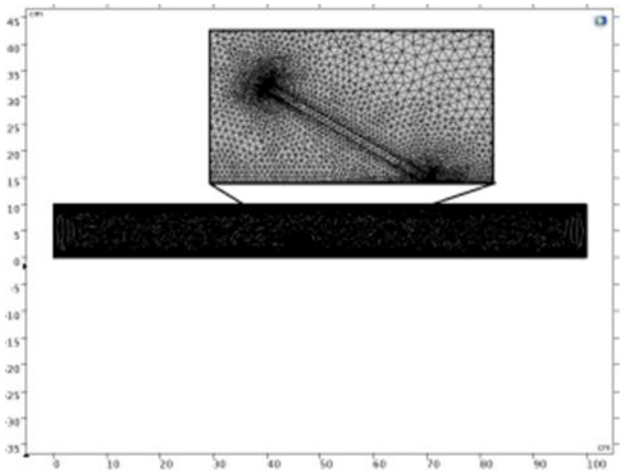

Figure 3. Mesh flow domain of the present problem.

RESULTS AND DISCUSSION

In the present numerical simulation, the nanofluids flow field supported out numerically has been equipped to confirm the Al_2O_3-water nanofluid flow appearances of the thin plate attached on the horizontal bottommost surface of the nanofluid flow duct with a height of H=10 cm and length of L=100 cm with obstacle thin plate with a height of 5 cm and a thickness of 0.5 cm placed in the middle of the channel. The assembly of the flow around the thin plate obstacle was confirmed at a Reynolds number of $Re = 4 \cdot 10^4$. The pressure distribution results in the channel are shown in Fig.4. The pressure varies with increasing the angle of the thin plate, where the pressure increased from 2.61 kPa to 6.21 kPa when increasing the plate angle from 30° to 90°. The inlet pressure changed from a low value in the case of the angle of inclination 30° and 60° of upstream angles and 120 and 150° of downstream angles. The high pressure of the inlet section is located at an inclination angle of 90° due to the blocked flow stream of the Al_2O_3-water nanofluid.

The results of the velocity contours were plotted in Fig.5. The Upstream of the obstacle thin plate, as the inclination angle in the upstream portion (30° and 60°), the flow was increased, and easy to pass the obstacle. But when the angle is put at 90°, a ratio of the Al_2O_3-water nanofluid remains choked, and a generation of small recirculation region is observed after the thin plate obstacle. However, in the downstream region of the thin plate obstacle, there is a great whirlwind, and the separation is activated. The results indicated that the thin plate obstacle in the flow field causes the separation of the fluid flow in the channel. The nanofluid flow field formulae a recirculation region near the thin plate, which increases the intensity of the turbulence due to increasing the angle of inclination from 30° to 90°. The velocity of the nanofluid grows progressively until it is attached to the near-back edge with the separation of the nanofluid flow. The length of the recirculation zone on the lower wall of the channel was indicated by the length near the thin plate, as mentioned in Fig.6. The results showed that the large area of separation developed behind the thin plate at an angle of inclination of 90°.

Heat transfer analysis

The effect of the thin plate angle of inclination on the temperature distribution in the channel is presented in Fig.S1 (Supplementary material). The results showed that increasing the thin plate angle of inclination led to decreasing the temperature in the upstream region of the thin plate from 31.02, 29.72, 29.17, 28.41, and 27.72 °C as increasing the angle of inclination from 30° to 150°, respectively, due to increasing the velocity of the nanofluid in this region. Also, the temperature in the downstream region of the thin plate increases from 30.27, 30.72, 31.42, 31.72, and 31.91°C as the inclination angle increases from 30° to 150°, respectively. Due to the decreasing velocity of the nanofluid in this region, the variation of the local Nusslet number of the heated lower surface of the channel with the increasing thin plate inclination angle was plotted in Fig.S2. The results indicated that the Nusslet number increased by 15 % when decreasing the angle from 90° to 30° and increasing by 8% when decreasing the angle from 90° to 60° in the region near the thin plate. The effect of increasing the nanoparticles' volume fraction on the local Nusselt number along the heated lower surface of the channel was illustrated in Fig. S3. The results indicated that increasing the nanoparticle volume fraction will increase the Nusslet number by about 10% when using Al_2O_3-water nanofluid instead of water.

Plate stresses analyses

Fig.S4 illustrates the geometry of the thin plate deformation of the thin plate and the stream at t = 4 s for various thin plate angles of inclination. The results indicated that a vortex exists for a small zone behind the thin plate obstacle when the flow and the moving thin plate system are near its steady state. The deformation magnitude, as well as the location and size of the vortex, are contingent on the magnitude of the velocity inflow and the thin plate angle of inclination. Therefore, the largest values of the mesh velocity are also near the thin plate. The results showed that the von Mises stress increased from 4.43×10^6 to 1.78×10^7 N/m when increasing the angle of inclination from 30° to 90°.

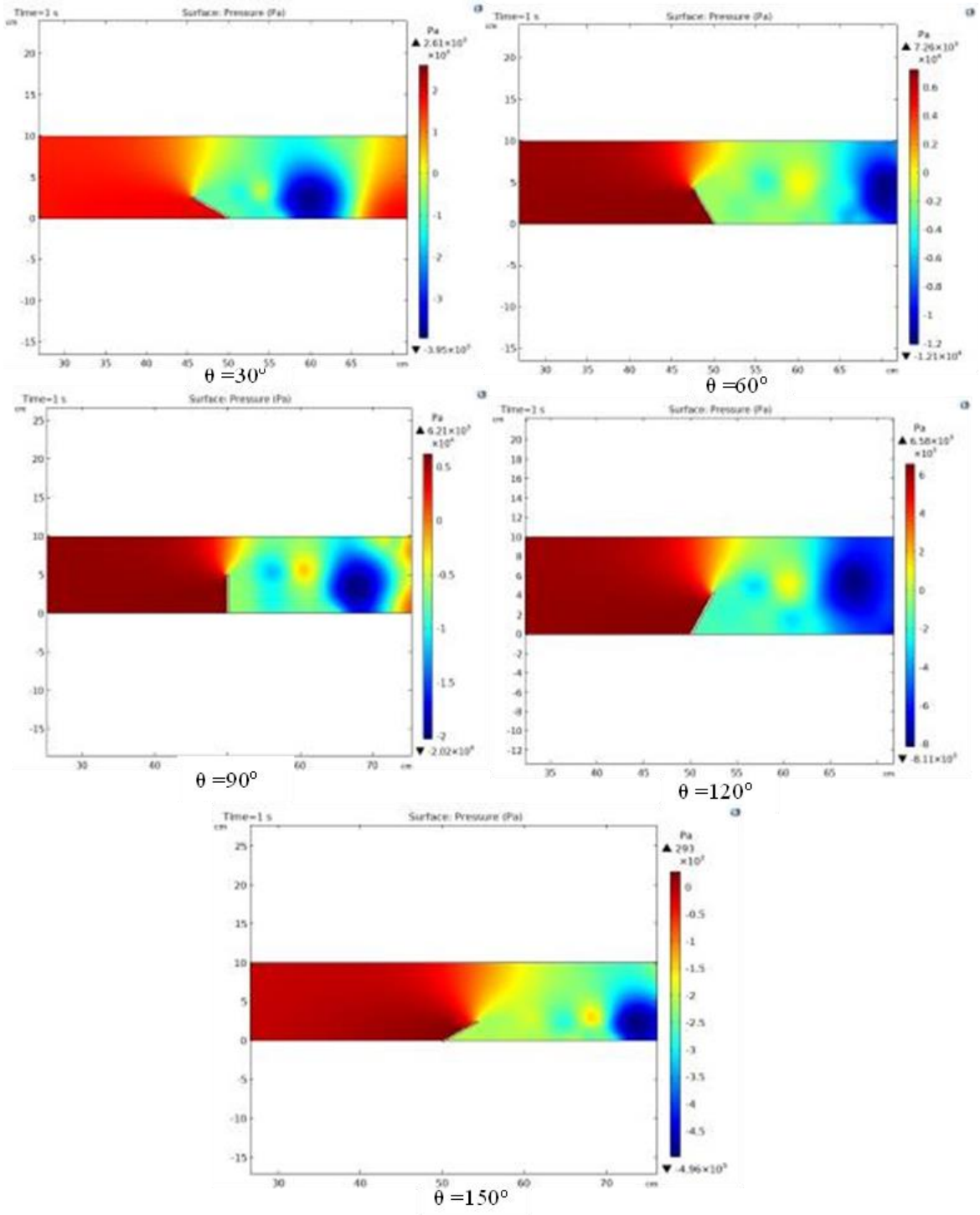

Figure 4. Nanofluid flow pressure for various thin plate obstacle angles at t = 4 s.

Whenever the angle of inclination starts to increase from 90° to 150°, the decrease of the thin plate deformation can be seen in the adverse velocity magnitude on the horizontal walls.

The effect of using different thin plate inclination angles on the drag force (left) and Y-displacement (right) with time was illustrated in Fig.S5. The outcomes display that the increasing the inclination angle from 30° to 90°, the maximum drag force will increase from 220 to 850 N/m; due to increasing the flow interception, the nanofluid flow and the thin plate will be perpendicular to the stream fluid flow in the case of the inclination angle of 90°.

Also, the X-displacement will have increased from 1.6 to 5.5 mm when increased the inclination angle from 30° to 90°. But the Y-displacement will decrease from 2.8 to 0 mm when the inclination angle increases from 30° to 90°.

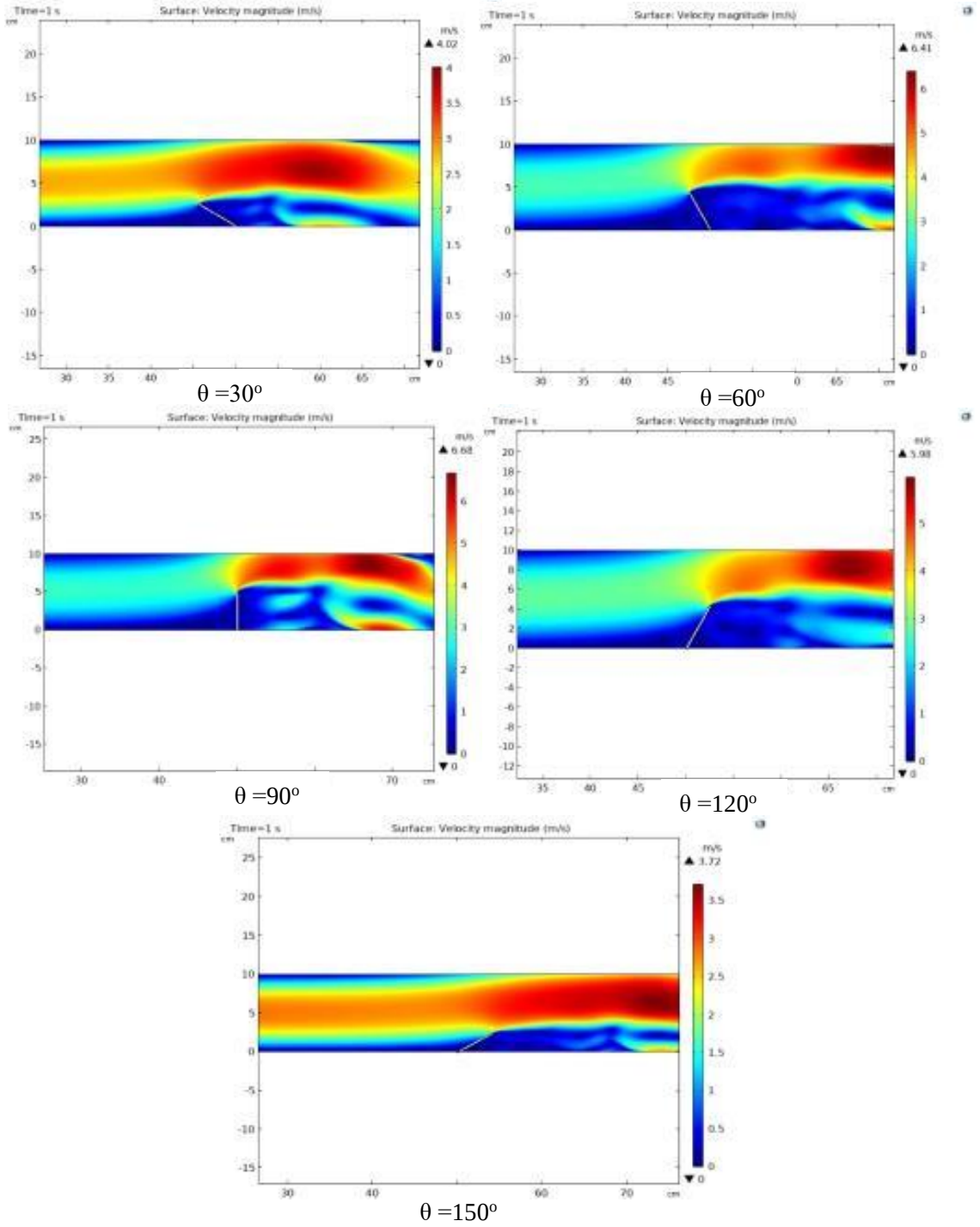

Figure 5. Nanofluid flow velocity for various thin plate obstacle angles at t = 4 s.

CONCLUSION

The numerical model presented in this simulation study is a 2D Al_2O_3-water nanofluid flow simulation by expanding the COMSOL Multiphysics 5.4 of turbulent flow around an inclined thin plate. The numerical results are presented as pressure contours, velocity contours, velocity vector, von Mises deformation stress, X and Y-displacement, and drag force fields. The effect of the nanofluid flow characteristics on the inclined thin plate obstacle deformation as a function of the Reynolds number of $Re=4\times10^4$ has been calculated with k-ε turbulence models. The results showed that an inclined thin plate obstacle in the flow direction leads to an increased pressure drop, von Mises deformation stress, X-displacement field, and drag force field. Also, increasing the inclined thin plate will increase these variables of the flow due to the interface between vortex

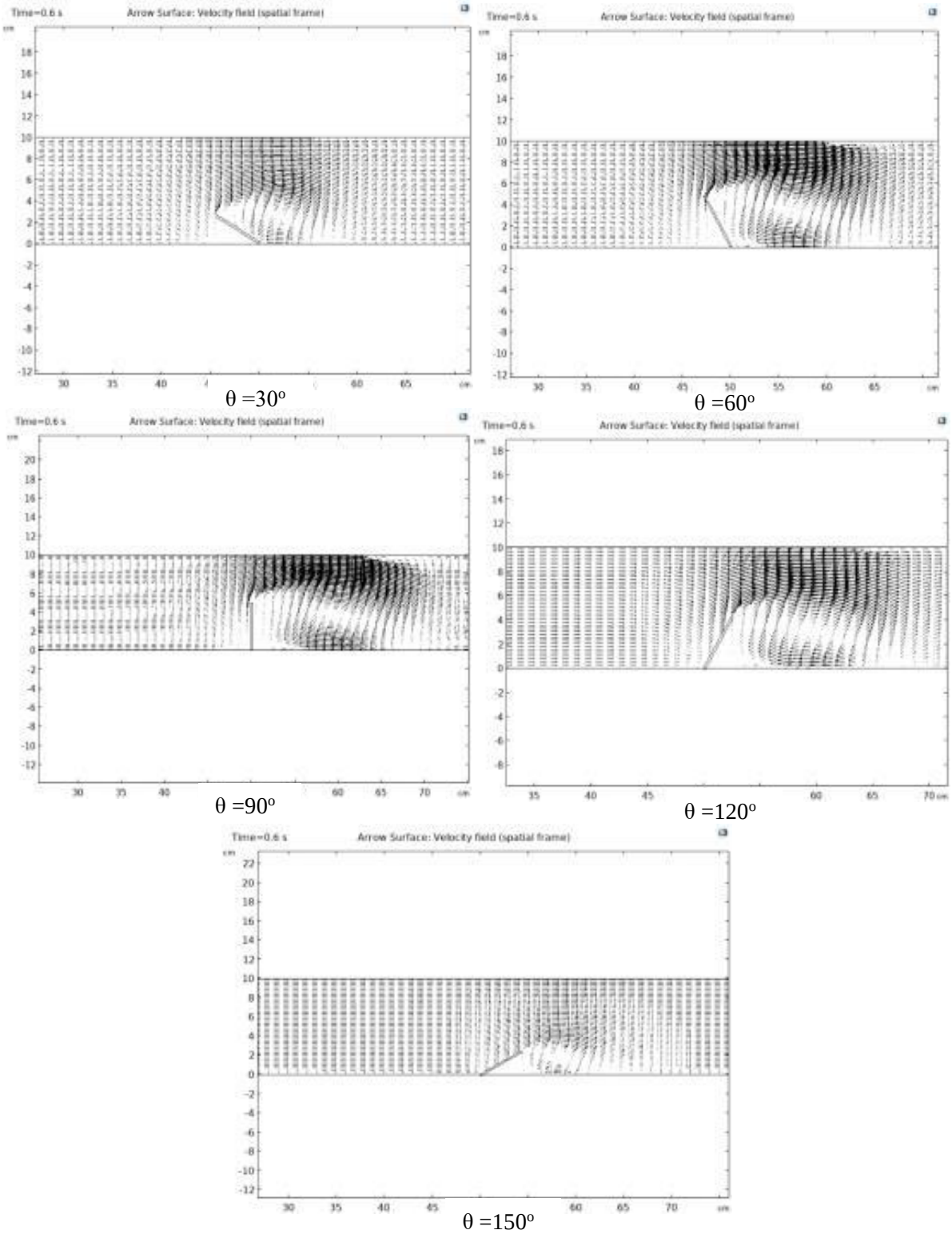

Figure 6. Nanofluid flow velocity vector for various thin plate obstacle angles at t = 4 s.

recirculation of the main nanofluids flow producing high recirculation vortex zones behind the thin plate. The result indicated that the Nusslet number increased by 15 % when the angle decreased from 90° to 30°. However, the results indicated that increasing the nanoparticle volume fraction will increase the Nusslet number by about 10% when using Al_2O_3-water nanofluid instead of water. In addition, the pressure increased from 2.61×10^3 to 6.21×10^3 Pa, the von Mises stress increased from 4.43×10^6 to 1.78×10^7 N/m, and

the X-displacement increased from 1.6 to 5.5 mm when increasing the plate angle from 30 to 90°.

NOMENCLATURE

I	The matrix of unit sloping
F	Force of volume disturbing of Al_2O_3-water nanofluid
n	Formal vector on a flat plate
Cp	Fanofluid specific heat capacity (J/kg K)
d	Particle diameter (m)
Dh	Hydraulic diameter (m)
f	Fluid friction factor (-)
Q	Fluid volumetric flowrate (m^3/s)
k	Thermal conductivity (W/m K)
k_B	Boltzmann constant (1.38×10^{-23}J/K)
L	Duct length (m)
P	Pressure (Pa)
PP	Pumping power (W)
Pe	Peclet number (-)
Qh	Heat flux (W)
Re	Reynolds number (-)
u	Fluid velocity (m/s)
x	Distance along duct cross section (m)
t	Time (sec)

Greek symbols

β	Thermal expansion coefficient, (1/K)
ϕ	Particle volume fraction (-)
μ	Viscosity (Pa.s)
ρ	Density (kg/m^3)

REFERENCES

[1] A. Okajima, T. Matsumoto, S. Kimura, JSME Int. J., Ser. B 41(1998) 214. https://doi.org/10.1299/jsmeb.41.214.

[2] J. Carberry, J. Sheridan, D.O. Rockwell, J. Fluids Struct. 15 (2001) 523–532. https://doi.org/10.1006/jfls.2000.0363.

[3] T. Sarpkaya, J. Fluids Struct. 19 (2004) 389–447. https://doi.org/10.1016/j.jfluidstructs.2004.02.005.

[4] X. Mao, Yu. Zhibin, Æ. Artur, J. Jaworski, D. Marx, Exp. Fluids 45 (2008) 833–846. https://doi.org/10.1007/s00348-008-0503-7.

[5] M. Dahl Jason, Ph.D. Thesis, Massachusetts Institute of Technology, (2008). http://hdl.handle.net/1721.1/44747.

[6] L. Lee, D. Allen, J. Fluids Struct. 26 (2010) 602–610. https://doi.org/10.1016/j.jfluidstructs.2010.02.002.

[7] X. Amandolèse, P. Hémon, Comptes Rendus Mécanique 338 (2010) 12–17. https://doi.org/10.1016/j.crme.2009.12.001.

[8] Y. Yang, M.Sc. Thesis, The Texas A&M University (2010).

[9] K. Lam, J.C. Hu, P. Liu, Phys. Fluids 22 (2010) 015105. https://doi.org/10.1063/1.3291069.

[10] B. Shrestha, S.N. Ahsan, M. Aurelia, Phys. Fluids 30 (2018) 013102. https://doi.org/10.1063/1.5001330.

[11] S. Zhang, T. Ishihara, Ocean Eng. 163 (2018) 583–598. https://doi.org/10.1016/j.oceaneng.2018.03.060.

[12] X. Sun, Y. Zehua, L. Jiajun, K. Wen,H. Tian, Int. J. Heat Mass Transfer 128 (2019) 319–334. https://doi.org/10.1016/j.ijheatmasstransfer.2018.08.123.

[13] D. Yaseen, M.A. Ismael, Exp. Tech. 47 (2022) 37–46. https://doi.org/10.1007/s40799-022-00554-9.

[14] S. Ram, N. Ashok, MD. Shamshuddin, J. of Nanofluids 12 (2023) 777–785. https://doi.org/10.1166/jon.2023.1976.

[15] Usman, S. Shaheen, M.B. Arain, K. S. Nisar, A. Albakri, MD. Shamshuddin, F. O. Mallawi, C. Stud. in Ther. Eng. 41(2023) 102523. https://doi.org/10.1016/j.csite.2022.102523.

[16] MD. Shamshuddin, F. Mabood, W. A. Khan, G. R. Rajput, Heat Trans. 52 (2023) 854–873. https://doi.org/10.1002/htj.22719.

[17] S.O. Salawu, R.A. Kareem, M.D. Shamshuddin, S.U. Khan, Chem. Phys. Lett. 760 (2020) 138011. https://doi/10.1016/j.cplett.2020.138011.

[18] MD. Shamshuddin, P. S. Rao, S.O. Salawu and A.J. Chamkha, J. Proc. Mech. Eng. 236 (2022) 1877–1888. https://doi/10.1177/09544089221076918.

[19] B. C. Pak, Y. I. Cho, Exp. Heat Trans. 11 (1998) 151–170. https://doi.org/10.1080/08916159808946559.

[20] Y. Xuan, W. Roetzel, Int. J. Heat Mass Transfer 43 (2000) 3701–3707. https://doi.org/10.1016/S0017-9310(99)00369-5.

[21] H.C. Brinkman, J. of Chem. Phys. 20 (1952) 571–581. https://doi/10.1063/1.1700493.

[22] J.C. Maxwell, A Treatise on Electricity and Magnetism, 2nd ed., Clarendon Press, Oxford University, UK (1881).

[23] S.E. Maiga, B. Nguyen, C. Tam, G. Nicolas, R. Gilles, Superlattices and Microstructures 35 (2004) 543–557. https://doi/10.1016/j.spmi.2003.09.012.

KADHUM AUDAA JEHHEF[1]
MUSAAB KADEM RASHEED[2]
MOHAMED ABED AL ABAS SIBA[3]

[1]Technical Engineering College, Baghdad, Middle Technical University, Baghdad, Iraq

[2]Institute of Technology, Middle Technical University, Baghdad, Iraq

NAUČNI RAD

NUMERIČKA SIMULACIJA UTICAJA OSCILIRAJUĆE TANKE PLOČE NA PROTOK NANOFLUIDA U KANALU

Ova numerička studija ima za cilj da predstavi efekat oscilirajuće tanke ploče sa različitim uglovima nagiba na protok nanofluida Al_2O_3-vode i performanse prenosa toplote. Naredni rad uspostavlja metode za formiranje interakcija fluid-struktura uticajem nanofluida Al_2O_3-voda na 0,1-1,0% v/v na tankoj ploči pomoću programskog paketa COMSOL Multiphisics 5.4. Turbulentni model je rešen korišćenjem (k-ε) modela, a strujanje oko tanke ploče je potvrđen pri Rejnoldsovom broju $Re=4\times10^4$. To je primer kako interakcija protoka nanofluida može da izobliči strukture. Proučavano je turbulentno dvodimenzionalno, stacionarno i nestišljivo strujanje oko oscilirajuće tanke ploče sa nagnutim uglovima uzvodno i nizvodno, postavljene unutar horizontalnog kanala. Numerička studija obuhvata istraživanje uticaja pet uglova nagiba tanke ploče (30, 60, 90, 120 i 150°) na pritisak, brzinu i temperaturu nanotečnosti Al_2O_3-voda. Takođe, studija je predstavila profil otpora i silu na tankoj ploči uzrokovanu protokom tečnosti. Rezultati su pokazali da oscilujuća tanka ploča unutar pravca strujanja povećava pad pritiska, fon Mizesov deformacioni napon, x-pomeranje, polja sile otpora i Nuseltov broj. Tamo gde se pritisak povećao sa $2,61\times10^3$ na $6,21\times10^3$ pa, fon Mizesov napon se povećao sa $4,43\times10^6$ na $1,78\times10^7$ N/m, a x-pomeraj se povećao sa 1,6 na 5,5 mm pri povećanju ugla ploče sa 30 na 90°.

Ključne reči: interakcije fluid-struktura, Lagranž-Ojlerova tehnika, Multiphysics, nanofluid.